RAPID COMMUNICATIONS

PHYSICAL REVIEW B VOLUME 47, NUMBER 15 15 APRIL 1993-I

First-principles phase diagrams of pseudoternary chalcopyrite–zinc-blende alloys

Roberto Osório,* Z. W. Lu, S.-H. Wei, and Alex Zunger
National Renewable Energy Laboratory, Golden, Colorado 80401
(Received 19 October 1992)

The temperature-composition phase diagrams of the pseudoternary $(CuInSe_2)_{1-x}(ZnSe)_{2x}$ and $(ZnSnP_2)_{1-x}(GaP)_{2x}$ chalcopyrite–zinc-blende semiconducting alloys are obtained by a combination of first-principles total-energy calculations with a statistical-mechanics description of a spin-1 Hamiltonian. We find that (i) alloying with zinc blende sharply lowers the order-disorder transition temperature of the chalcopyrite, (ii) despite the different crystal structures of the constituents, the alloy exhibits miscibility already above ~ 500 K, and (iii) while the equilibrium ground state corresponds to phase separation, a *metastable* long-range-ordered intermediate stannite-type compound $CuInZn_2Se_4$ is predicted.

The $A^IB^{III}C_2^{VI}$ chalcopyrite compounds (e.g., $CuInSe_2$) form a diverse group of semiconducting materials.[1] They have been used widely in photovoltaic device applications,[2] but their properties at a fundamental level are relatively unknown. The chalcopyrite (CH) structure[3] can be viewed as a "natural superlattice" consisting of a two monolayer $(AC)_2/(BC)_2$ alternation along the [201] direction. At a critical temperature T_c, these compounds undergo a transition to a state where the A and B atoms are disordered on the cation sublattice,[4] thus forming a zinc-blende-like (ZB) $A_{0.5}B_{0.5}C$ alloy. Disordering is accompanied by a *reduction* of the band gap.[5] The transition temperature T_c usually increases with the A-B size mismatch[4] and is rather high (900–1300 K) in most chalcopyrites; in some cases, the CH compounds remain ordered at all temperatures below melting.[4] One can expect, however, that a CH→ZB transition will occur at a *fixed* lower temperature through alloying with a common-anion $D^{II}C^{VI}$ zinc-blende compound: If the two components are soluble, there will be a D-atom concentration above which this atom will have equal probability of occupying all sites of the cation sublattice, leading to a disordered (ZB) alloy. Since $D^{II}C^{VI}$ semiconductors always have a *larger* band gap than the equivalent[6] $A^IB^{III}C_2^{VI}$ chalcopyrite, such an alloying reaction will raise the band gap of $A^IB^{III}C_2^{VI}$. Interest in band-gap engineering of chalcopyrite semiconductors[7] has, therefore, focused on the question of mutual solubility with zinc-blende compounds.

Numerous CH-ZB alloys have been prepared by high-temperature melt-and-anneal techniques. These include the sulfide $CuGaS_2/ZnS$,[8] the selenides of $CuGaSe_2$ (Ref. 9) and of $CuInSe_2$ (Refs. 7 and 9) with ZnSe, as well as the tellurides of $CuGaTe_2$ with ZnTe (Ref. 10) and CdTe,[11] and of $CuInTe_2$ with ZnTe,[12] CdTe, and MnTe.[13] At high temperatures, the phase diagrams show large regions of solid solutions having either the CH or the ZB symmetry. However, low-temperature data are not available to determine if the CH-ZB system is inherently phase separating or ordering. Experience with other alloys whose components have different crystal structure (e.g., zinc-blende GaAs with diamondlike Ge) suggests limited equilibrium solubility and no intermediate ordered compounds. We present here the results of *ab initio* temperature-composition phase diagrams of a pseudoternary semiconductor system. We study the CH-ZB alloy $(CuInSe_2)_{1-x}(ZnSe)_{2x}$ and the "III-V analog" $(ZnSnP_2)_{1-x}(GaP)_{2x}$. We find that (i) alloying reduces dramatically the order-disorder temperature of the CH component and (ii) alloying produces regions of complete solid solubility well below melting, but (iii) at lower temperatures these systems phase separate, rather than order. (iv) For $(CuInSe_2)_{1-x}(ZnSe)_{2x}$, the ordered stannite (ST) structure,[3] a CuSe/ZnSe/InSe/ZnSe superlattice stacked along [201], appears as a *metastable* structure around $x \approx 1/2$. It should be observed if at low temperatures, only short-range atomic diffusion exists.

The problem is addressed in two steps. First, we consider the occupations of the fcc cation sublattice by A and B atoms in the $A^I_{0.5}B^{III}_{0.5}C^{VI}$ system. Second, we add the third cation D^{II} competing for the same sublattice. The common anion C resides on its own fcc sublattice and hence does not carry a statistical degree of freedom. (We neglect high-energy anion-cation antisite defects.) In addressing the first problem we consider the spin-1/2 Ising model where site i is occupied by either an A atom ($\sigma_i = -1$) or by a B atom ($\sigma_i = +1$). We take the Ising Hamiltonian for an arbitrary configuration $\boldsymbol{\sigma}$ of this binary system to be

$$\mathcal{H}_{\rm bin}(\boldsymbol{\sigma}) = \tilde{J}_0 + \sum_{(ij)} J_{ij}\sigma_i\sigma_j + \sum_{(ijkl)} J_{ijkl}\sigma_i\sigma_j\sigma_k\sigma_l \,, \qquad (1)$$

where (ij) indicates a summation over all pairs, and $(ijkl)$ indicates a summation over all tetrahedra in the lattice. To find the values of the interaction parameters $\{J\}$ we fit Eq. (1) to a set of directly calculated local-density approximation (LDA) formation enthalpies $\Delta H(\boldsymbol{\sigma})$ of simple AC/BC ordered structures at the equi-

librium volume. The practical completeness of the expansion is then examined by the ability of this set $\{J\}$ to predict via Eq. (1) the energies $\Delta H(\boldsymbol{\sigma}')$ of other structures $\boldsymbol{\sigma}'$ not used in the fit. For example, we have used LDA to calculate $\Delta H(\boldsymbol{\sigma})$ for six equimolar $(\mathrm{CuSe})_p(\mathrm{InSe})_p$ short-period ($p = 1, 2$) superlattices, *not including the chalcopyrite structure*. Retaining in Eq. (1) only the empty-site energy $\tilde{J}_0$ and the nearest-neighbor pair interaction J_2 produces a prediction of $\Delta H(\mathrm{CH}) = -1183.4$ meV/cation compared with the LDA value $\Delta H(\mathrm{CH}) = -1163.0$ meV/cation. This 20-meV prediction error can be reduced to 0.4 meV if the nearest-neighbor four-body term J_4 is added. Further addition of second-, third-, and fourth-neighbor pair interactions J_{ij} lead to a similar prediction error of 0.25 meV. We thus choose to retain only $\tilde{J}_0$, J_2, and J_4 in the Hamiltonian of Eq. (1). Fitting these parameters to the $\Delta H(\boldsymbol{\sigma})$ of seven superlattices results in the J_2 and J_4 values given in Table I. The dominant interaction $J_2 > 0$ shows that the $A^{\mathrm{I}}_{0.5}B^{\mathrm{III}}_{0.5}C^{\mathrm{VI}}$ system is compound-forming (or "antiferromagnetic"). The order-disorder transition obtained in a Monte Carlo (MC) simulation for $CuInSe_2$ is $T_c = 1120$ K, in perfect agreement with the earlier result[5(a)] using up to fourth-neighbor pair interactions. The cluster-variation method (CVM) tetrahedron approximation leads to $T_c = 1224$ K. The four-body term J_4 acts to lower T_c by as much as 300 K in both the MC and the CVM calculations. We will hence proceed using CVM with the interaction energies given in Table I.

The consideration of the pseudoternary case $(ABC_2)_{1-x}(DC)_{2x}$ requires two changes. First, a generalization to a spin-1 Hamiltonian, representing occupations of site i by A ($S_i = 1$), B ($S_i = -1$), and D ($S_i = 0$), is needed. Second, the added interaction terms are now *volume dependent* since the end-point chalcopyrite and zinc-blende constituents can have different equilibrium molar volumes,[14] in contrast to the pseudobinary case, where all structures $(\mathrm{CuSe})_p(\mathrm{InSe})_p$ had the same composition and, hence, nearly equal molar volumes. We will therefore use a nearest-neighbor spin-1 Ising model (a generalized Blume-Emery-Griffiths,[15] or BEG, model) with volume-dependent interactions:

$$\mathcal{H}_{\mathrm{tern}}(\mathbf{S}, V) = \left[J_2 \sum_{\langle ij \rangle} S_i S_j + J_4 \sum_{\langle ijkl \rangle} S_i S_j S_k S_l\right] + J_0(V) + D(V) \sum_i S_i^2 - K(V) \sum_{\langle ij \rangle} S_i^2 S_j^2 \,. \tag{2}$$

The terms in brackets are the nearest-neighbor terms of Eq. (1), with the interactions given in Table I. All odd terms were omitted, assuming that the Hamiltonian is invariant under the $A \leftrightarrow B$ interchange. This was found to be a good approximation in the ternary system $(\mathrm{GaAs})_{1-x}\mathrm{Ge}_{2x}$.[18]

Using the linear-augmented-plane-wave (LAPW) method,[16] we have calculated the volume-dependent total energies E_S for structures $S =$ ZB, CH, and ST, finding also the equilibrium volumes V_S. Interpolating these volumes we get $V(x)$. The functions $J_0[V(x)]$, $D[V(x)]$, and $K[V(x)]$ are then obtained by fitting Eq. (2) to the three LAPW equations of state $E_S(V)$, keeping J_2 and J_4 constant. The basic trends in the results can be assessed by considering the *excess* energies $\Delta E_S(V) = E_S(V) - (1-x)E_{\mathrm{CH}}(V_{\mathrm{CH}}) - xE_{\mathrm{ZB}}(V_{\mathrm{ZB}})$. In terms of our basic parameters,

$$\Delta E_{\mathrm{ST}}(V) = (2K - J_4) + g(V) \,, \tag{3a}$$

$$\Delta E_{\mathrm{rand}}(V) = (2K + J_2 - J_4) + g(V) - K(V)/2 \tag{3b}$$

for the $x = 1/2$ stannite and random alloy, respectively. Here, quantities without an argument refer to $V = V_{\mathrm{CH}}$ and $g(V) \equiv \Delta J_0(V) + \Delta D(V)/2 - \Delta K(V) - \Delta J_0(V_{\mathrm{ZB}})/2$, where $\Delta f \equiv f(V) - f(V_{\mathrm{CH}})$. The "volume deformation" (VD) energy of the constituents, $[\Delta E_{\mathrm{CH}}(V) + \Delta E_{\mathrm{ZB}}(V)]/2$ is

$$\Delta E_{\mathrm{VD}}(V) = g(V) - 2\Delta K(V) \,. \tag{4}$$

Figure 1 depicts the excess energies of Eqs. (3) and (4), at $x = 1/2$, and Table I summarizes the pertinent constants. The following trends appear: (i) The formation enthalpy of the stannite structure $\Delta H_{\mathrm{ST}} \equiv \Delta E_{\mathrm{ST}}(V_{\mathrm{ST}})$ is positive. Hence this structure is globally unstable towards decomposition into its *equilibrium* CH and ZB constituents, at V_{CH} and V_{ZB}, respectively. This comes about due to $2K - J_4 + g(V_{\mathrm{ST}}) > 0$ (Table I). (ii) Nevertheless, the $CuInZn_2Se_4$ stannite structure is stabler than CH + ZB, where both constituents are held at $V = V_{\mathrm{ST}}$, i.e., $\delta E^{\mathrm{VD}}_{\mathrm{ST}} \equiv \Delta E_{\mathrm{ST}} - \Delta E_{\mathrm{VD}} < 0$. The opposite is true for $(\mathrm{ZnSnP_2})_{1-x}(\mathrm{GaP})_{2x}$. (iii) For both systems, the "ordering" energy $\delta E^{\mathrm{ord}}_{\mathrm{ST}} \equiv \Delta E_{\mathrm{ST}} - \Delta E_{\mathrm{rand}} = -J_2 + K(V)/2$ is negative (since $J_2 \gg 0$). Conclusion (i) implies that, at low-temperature, both systems will acquire the phase-separating equilibrium state. Conclusions (ii) and (iii) imply that in $(\mathrm{CuInSe_2})_{1-x}(\mathrm{ZnSe})_{2x}$ the stannite structure is stable towards *local* phase separation ($\delta E^{\mathrm{VD}}_{\mathrm{ST}} < 0$) and randomization ($\delta E^{\mathrm{ord}}_{\mathrm{ST}} < 0$). It should hence appear as a metastable ordered phase at low temperatures. In contrast, the stannite structure $ZnSnGa_2P_4$ is unstable relative to local phase separation.

Newman and Xiang[19] have previously performed model calculations using a simplified version of the

TABLE I. Interaction parameters (in meV) and excess energies (in meV/cation) for $(\mathrm{CuInSe_2})_{1-x}(\mathrm{ZnSe})_{2x}$ (CIS) and $(\mathrm{ZnSnP_2})_{1-x}(\mathrm{GaP})_{2x}$ (ZSP).

	J_2	J_4	K	$g(V_{\mathrm{ST}})$	$\tilde{K}$	ΔH_{ST}	$\delta E^{\mathrm{VD}}_{\mathrm{ST}}$	$\delta E^{\mathrm{ord}}_{\mathrm{ST}}$
CIS	70	8	5	10	10	13	-0.3	-68
ZSP	79	11	15	-8	11	10	2	-75

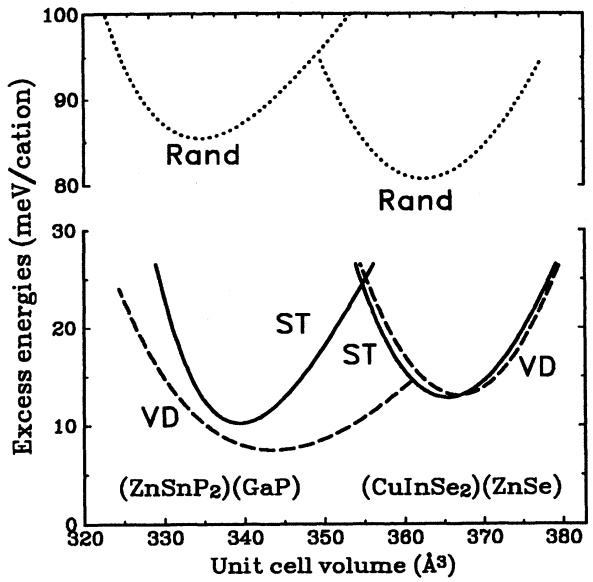

FIG. 1. Volume dependence of the excess energies of the stannite structure (ST), volume deformation (VD), and of the random alloy, of $(CuInSe_2)_{0.5}(ZnSe)_{0.5}$ and of $(ZnSnP_2)_{0.5}(GaP)_{0.5}$. The energy zero is $[E_{CH}(V_{CH}) + E_{ZB}(V_{ZB})]/2$.

Hamiltonian of Eq. (2), with $J_4 = \Delta J_0 = \Delta K = \Delta D = 0$. Mapping the CVM solutions in the parameter range $-1 \leq K/J_2 \leq 0$, they found a variety of interesting ordered and partially-ordered phases. Since we find that, for $(CuInSe_2)_{1-x}(ZnSe)_{2x}$ and $(ZnSnP_2)_{1-x}(GaP)_{2x}$, (i) $K/J_2 > 0$, (ii) J_4 is an important contribution to the Hamiltonian, and (iii) volume dependence is significant, their results are not directly applicable to the systems considered here.

We solved the statistical mechanics of Eq. (2) in the CVM tetrahedron approximation. The CVM solution is based on expressing the configurational lattice entropy S as a function of occupation variables, i.e., probabilities of different configurations of the basic cluster (in this case a tetrahedron) and its subclusters. Statistical correlations inside the tetrahedron cluster are correctly described, but longer-range correlations, present in MC simulations, are neglected. We have therefore scaled down our CVM temperature approximately by $T_{MC}/T_{CVM} = 0.92$, obtained from calculations on the pseudobinary ABC_2 system (including both J_2 and J_4). At each composition and temperature, the CVM free energy $F = \mathcal{H}_{tern} - TS$ is minimized with respect to the occupation variables, using the "natural iteration"[17] procedure, and with respect to the molar volume V.

Figure 2 shows the calculated phase diagrams of $(CuInSe_2)_{1-x}(ZnSe)_{2x}$, using a hierarchy of approximations in the Hamiltonian of Eq. (2): (i) J_2 only, (ii) J_2 and K, (iii) J_2, K, and J_4, (iv) volume-dependent interaction-energies. In cases (ii) and (iii) we used the value $\tilde{K} \equiv K + g(V_{ST})/2 = 10.5$ meV for K, corresponding to a fit of the BEG Hamiltonian to the equilibrium-volume energies of the CH, ST, and ZB structures. The diagram of case (i) corresponds to the antiferromagnetic spin-1 Ising model in the fcc sublattice and reproduces the $K = 0$ figure of Newman and Xiang,[19] except for a richer account of details presented here just above the triple point at $T_{tr} \approx 390$ K (namely, a miscibility gap within the chalcopyrite phase and a small miscibility gap between the chalcopyrite and the zinc-blende phases). The diagram of case (ii) shows the role of positive K values: it widens the CH-ZB miscibility gaps, suppressing the small second-order transition line present in case (i) between ≈ 410 and 550 K, and removes the triple point. The diagram of case (iii) shows that J_4 acts to reduce considerably the transition temperatures in the low-x region and to reduce the width of the CH-ZB miscibility gap. Finally, the use of the most accurate model with volume-dependent interactions acts to increase the CH-ZB miscibility gap [Fig. 2(b)]. The maximum equilibrium solubility of ZnSe in $CuInSe_2$ with the chalcopyrite structure is 22% (at $T \approx 770$ K), while $CuInSe_2$ becomes completely soluble in ZnSe with the zinc-blende structure above the order-disorder temperature of $CuInSe_2$. Our results hence show that, contrary to the other known heterostructural ternary alloy $(GaAs)_{1-x}Ge_{2x}$,[20] characterized by vanishing equilibrium solid solubility, $(CuInSe_2)_{1-x}(ZnSe)_{2x}$ exhibits

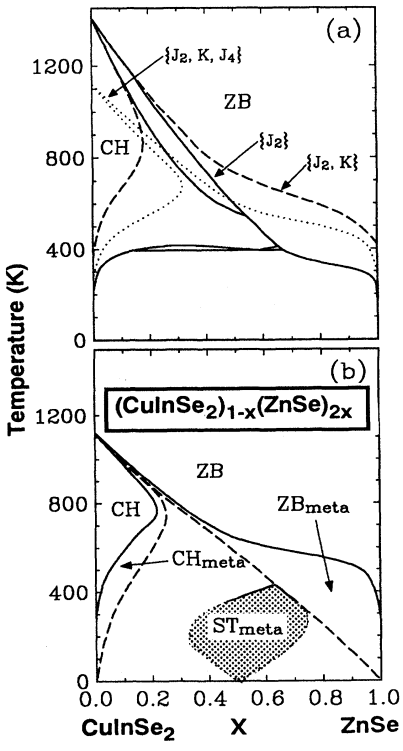

FIG. 2. Phase diagrams of $(CuInSe_2)_{1-x}(ZnSe)_{2x}$, showing the chalcopyrite (CH) and zinc-blende (ZB) phases, for different interaction models. (a) Dotted lines: $J_2 = 70$, $J_4 = 8$, $K = 10$ meV. Dashed lines: imposing $J_4 = 0$. Solid lines: imposing $J_4 = K = 0$. (b) Using volume-dependent interactions. In the metastable stannite (ST_{meta}) region, the solid lines are the result of the CVM calculations; the shaded region includes a qualitative extrapolation to the lower temperatures.

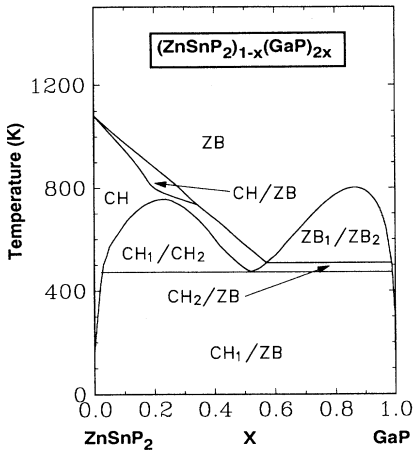

FIG. 3. First-principles phase diagram of $(ZnSnP_2)_{1-x}(GaP)_{2x}$, using volume-dependent interactions. The different regions are described in the text.

substantial solubility. Additional metastable features are presented for this *ab initio* phase diagram. The left dashed line in Fig. 2(b) marks the chalcopyrite spinodal, which is the upper-composition limit of metastability for the CH phase. The right dashed line is the unstable second-order transition line inside the coexistence region and marks the lower-composition limit for metastability of the zinc-blende phase. Between these two lines we find $\partial^2 F/\partial x^2 < 0$, which implies that any incipient phase separation will be preferred to a single-phase state. Since at $x = 1/2$ we found $0 < \Delta H(\mathrm{ST}) < \Delta E_{\mathrm{VD}} < \Delta E_{\mathrm{rand}}$ (Fig. 1), the stannite structure could be observed in $(CuInSe_2)_{1-x}(ZnSe)_{2x}$ if *long-range* atomic diffusion were inhibited. The shaded region at $x \sim 1/2$, $T < 440$ K shows this marginally *metastable ST* phase. It should be observed if *short-range* atomic rearrangements are allowed but *long-range* atomic migration (and hence, phase separation) is slow at $T < 440$ K. The chalcopyrite-forbidden x-ray diffraction peaks at (001), (110), (112), and (221) $\times 2\pi/a$ characterize the ST phase. Calorimetric and magnetic-susceptibility measurements in $(A^{\mathrm{I}}B^{\mathrm{III}}\mathrm{Te}_2)_{1-x}(\mathrm{MnTe})_{2x}$ alloys have indicated two low-temperature phases described by ordering of the Mn atoms.[13] Although the structure of these phases is still unknown (the above mentioned x-ray peaks were not measured) the structure called "chalcopyrite-ordered"[13] could be stannitelike.

Figure 3 shows the phase diagram obtained for $(ZnSnP_2)_{1-x}(GaP)_{2x}$. Miscibility gaps are obtained inside the chalcopyrite (CH_1/CH_2) and the zinc-blende (ZB_1/ZB_2) phases and between $x \sim 1/2$ chalcopyrite and zinc blende (CH_2/ZB). These new features are caused in part by the larger volume deformation effects in this alloy: the lattice mismatch is 3.6% as opposed to 2.1% in $(CuInSe_2)_{1-x}(ZnSe)_{2x}$. A stronger volume dependence of the $g(V)$ term in Eqs. (3) and (4) results at ~ 600 K in lower free energies of the chalcopyrite and zinc-blende phases at $x \sim 1/2$ than at $x \sim 0$ or $x \sim 1$, which provokes the two miscibility gaps. The stannite phase is, however, unstable both globally ($\Delta H_{\mathrm{ST}} > 0$) and locally ($\delta E_{\mathrm{ST}}^{\mathrm{VD}} > 0$).

In conclusion, we have demonstrated that *ab initio* methods can be used to obtain rich phase diagrams of pseudoternary semiconducting alloys, including regions of chalcopyrite and zinc-blende stability, miscibility gaps, and regimes of metastability of intermediate ordered phases. This provides guidelines for searching ordering in these technologically important semiconductors. It also opens the door to the study of more complex nonstoichiometric pseudoternary compounds, like $(In_{1-y}Ga_yP)_{1-x}(AlP)_{2x}$.

This work was supported in part by the U.S. Department of Energy, Office of Energy Research, Basic Energy Science Grant No. DE-AC02-83CH10093.

*Permanent address: Departamento de Física, Universidade de Brasília, 70910 Brasília, Distrito Federal, Brazil.

[1] J. L. Shay and J. H. Wernick, *Ternary Chalcopyrite Semiconductors* (Pergamon, Oxford, 1975).

[2] *Copper Indium Diselenide for Photovoltaic Applications*, edited by T. J. Coutts, L. L. Kazmerski, and S. Wagner (Elsevier, New York, 1986).

[3] E. Parthé, *Crystal Chemistry of Tetrahedral Structures* (Gordon and Breach, New York, 1964) shows the structures of $CuFeS_2$ chalcopyrite (p. 37) and of Cu_2FeSnS_4 stannite (p. 44).

[4] A. Zunger, Appl. Phys. Lett. **50**, 164 (1987).

[5] (a) S. H. Wei, L. G. Ferreira, and A. Zunger, Phys. Rev. B **45**, 2533 (1992); (b) C. Rincón, *ibid.* **45**, 12 716 (1992).

[6] J. E. Jaffe and A. Zunger, Phys. Rev. B **29**, 1882 (1984).

[7] J. N. Gan *et al.*, Phys. Rev. B **12**, 5797 (1975); W. Gebicki, M. Igalson, and R. Trykozko, Acta Phys. Pol. A **77**, 367 (1990).

[8] A. Ooe and S. Iida, Jpn. J. Appl. Phys. **29**, 1484 (1990).

[9] V. G. Lambrecht, Mat. Res. Bull. **8**, 1383 (1973).

[10] L. Garbato, F. Ledda, and P. Manca, Jpn. J. Appl. Phys. Suppl. **19-3**, 67 (1980).

[11] A. Aresti *et al.*, J. Electrochem. Soc. **124**, 766 (1977).

[12] C. Neal *et al.*, J. Phys. D **22**, 1347 (1989).

[13] M. Quintero *et al.*, J. Solid State Chem. **87**, 456 (1990).

[14] The LDA equilibrium lattice constants are 5.747 Å for $CuInSe_2$ ($c/a = 1.01$) and 5.614 Å for ZnSe, compared with the experimental values of 5.785 ($c/a = 1.00$) and 5.668 Å, respectively.

[15] M. Blume, V. J. Emery, and R. B. Griffiths, Phys. Rev. A **4**, 1071 (1971).

[16] S.-H. Wei and H. Krakauer, Phys. Rev. Lett. **55**, 1200 (1985).

[17] R. Kikuchi, J. Chem. Phys. **60**, 1071 (1974).

[18] R. Osório and S. Froyen, Phys. Rev. B **47**, 1889 (1993).

[19] K. E. Newman and X. Xiang, Phys. Rev. B **44**, 4677 (1991).

[20] R. Osório, S. Froyen, and A. Zunger, Solid State Commun. **78**, 249 (1991).